Anal. Methods Environ. Chem. J. 5 (2) (2022) 39-50

AMECJ

Research Article, Issue 2
Analytical Methods in Environmental Chemistry Journal
Journal home page: www.amecj.com/ir

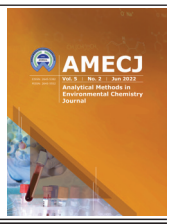

Response surface modeling for the treatment of methylene blue from aqueous media using electro-Fenton process before determination by UV-Vis spectrometer: Kinetic and degradation mechanism

Sara Zahedi [a], Ali Asadipour [b], Maryam Dolatabadi [c], Saeid Ahmadzadeh [d, e, *]

[a] *Student Research Committee, Kerman University of Medical Sciences, Kerman, Iran.*
[b] *Department of Medicinal Chemistry, Faculty of Pharmacy, Kerman University of Medical Sciences, Kerman, Iran.*
[c] *Environmental Science and Technology Research Center, Department of Environmental Health Engineering, School of Public Health, Shahid Sadoughi University of Medical Sciences, Yazd, Iran.*
[d] *Pharmaceutics Research Center, Institute of Neuropharmacology, Kerman University of Medical Sciences, Kerman, Iran.*
[e] *Pharmaceutical Sciences and Cosmetic Products Research Center, Kerman University of Medical Sciences, Kerman, Iran*

ARTICLE INFO:

Received 3 Mar 2022
Revised form 29 Apr 2022
Accepted 16 May 2022
Available online 29 Jun 2022

Keywords:
Electro-Fenton process,
UV-Vis spectrometer,
Methylene blue,
Response surface methodology,
Degradation,
Kinetic

ABSTRACT

In the present study, response surface methodology was employed to investigate the effects of main variables, including the initial MB concentration, hydrogen peroxide dosage, current density, and electrolysis time on the removal efficiency of MB using the electro-Fenton (EF) process. The MB concentration determination by UV-Vis spectrometer**.** The EF process degrades the MB contaminant molecules by the highly oxidizing species of the ·OH. A quadratic regression model was developed to predict the removal of MB, where the R^2 value was found to be 0.9970, which indicates the satisfactory accuracy of the proposed model. ANOVA analysis showed a non-significant lack of fit value (0.0840). Moreover, the predicted correlation coefficient values (R^2=0.9915) were reasonably in agreement with the adjusted correlation coefficient value (R^2=0.9958), demonstrating a highly significant model for MB dye removal. In addition, the obtained results showed 95.8% MB was removed in the optimum removal efficiency, including the initial MB concentration of 20 mg L^{-1}, H_2O_2 dosage of 400 µL, and the current density of 7.0 mA cm^{-2}, and electrolysis time of 10 min which was agreed with the predicted removal efficiency of 98.3%. Electrical energy consumption was found to be 0.163 kWh m^{-3}. The constant rate value of K_{app} at the optimum operating condition was 0.3753 min^{-1}.

1. Introduction

Due to the increasing use of tens of thousands of various types of dyes, which are employed in plastic products, cosmetics, leather, and food industries, and their release of about over 100 tons into the aqueous environments, a severe global concern has been raised for efficient removal of such organic micropollutants before releasing the industrial wastewater into the environmental medium [1, 2]. The adverse effects of toxic dyes on human beings, biota, microorganisms, and environmental health, even at deficient concentrations on the one hand, and their high resistance to photochemical and biological degradation, on the other hand, the

*Corresponding Author: Saeid Ahmadzadeh
Email: saeid.ahmadzadeh@kmu.ac.ir
https://doi.org/10.24200/amecj.v5.i02.178

necessity has required to eliminate the synthetic dyes contaminant from effluents [3-5]. Among the high-consumption dyes, methylene blue (MB), a derivative of phenothiazine, is widely used as a redox indicator, biological staining reagent, medication to treat methemoglobinemia, and adjunct employed in endoscopic polypectomy. Besides, it is used extensively in textiles dyeing industries of cotton, wool, and silk. Exposure of methylene blue to the eyes causes irreversible damage of partial blindness [6, 7]. Moreover, its inhalation causes respiratory problems. Its ingestion orally causes a burning sensation in the gastrointestinal tract and induces nausea, vomiting, profuse sweating, as well as mental confusion, and methemoglobinemia [8-11]. There are many techniques such as UV-VIS spectrometer, gas chromatography, and liquid chromatography for determining MB, dye, tyrosine kinase, toluene, benzene, and organic materials in different matrixes [12-17]. During the last decades, several treatments techniques, including coagulation, adsorption, and filtration processes, have been developed for the removal of dye contaminants which suffered from the disadvantages such as high operational costs due to the production of a massive amount of sludge or solid waste and transferring the dyes to another phase by concentrating them rather than eliminating them [18, 19]. The advanced oxidation processes (AOPs) as an economical and high efficient approach provide a valuable opportunity to overcome the limitations of the conventional treatment process by generating a robust oxidative agent of hydroxyl radicals, which degrade and mineralize the dye molecules into their less-toxic forms and harmless inorganic products such as water or carbon dioxide [20-22]. As seen from the proposed reaction in Equation 1, Fenton's reagent of Fe^{2+} and H_2O_2 generates the oxidative agents of hydroxyl radicals under the acidic medium of solution pH less than 3. The Fe^{2+} species are generated from the oxidation of iron anode electrode and reduction of Fe^{3+} ions through cathodic reaction as described by Equation 2 [23, 24].

$$Fe^{2+} + H_2O_2 \rightarrow Fe^{3+} + OH^- + HO^\bullet$$

(Fenton's reaction) (Eq. 1)

$$Fe^{3+} + e^- \rightarrow Fe^{2+} \ (E^\circ = 0.77 \text{ V/SHE})$$ (Eq. 2)

In the current work, response surface methodology (RSM) was employed as a computational approach to optimize the removal efficiency of MB using the EF process. The effect of main operational variables, including electrolysis time, MB initial concentration, H_2O_2 dosage, and current density throughout the treatment process, were evaluated, and the kinetics of the process were studied.

2. Material and methods

2.1. Chemical

All chemicals used in the MB removal study are analytical (high purity) grade without further purification. $C_{16}H_{18}ClN_3S$ (Methylene blue), H_2O_2 (30%, v/v), Na_2SO_4, H_2SO_4, and NaOH were obtained from Merck® Co. $(CH_3)_3COH$, and CH_3OH were obtained from Sigma Aldrich® Co. The investigation samples in this study were prepared in double-distilled water (DDW).

2.2. EF process system

The Pyrex cylindrical reactor with dimensions of 9.0 cm (height) × 7.0 cm (diameter) and a volume capacity of 300 mL was used to carry out MB removal studies using the EF process. The iron electrodes with a thickness of 0.1 cm and an immersed area of 12 cm^2 were used as cathode and anode electrodes. The distance between electrodes (anode and cathode) was considered constant and equal to 3.0 cm. In a typical run, MB solution was degraded in the reactor with 50 mM Na_2SO_4 as the supporting electrolyte. The pH of the MB solution was adjusted to 3.0 by 0.01 M of H_2SO_4. The rotation speed was kept at 200 rpm during the experiment.

2.3. Analytical methods

The MB concentration of samples before and after the treatment process was measured by a UV-

Vis spectrometer (OPTIZEN 3220 model) at 670 nm [1]. Evaluations for the degradation and MB removal efficiency and total amount of electrical energy consumption (kWh m^{-3}) were calculated from the Equation (3) and (4) [25-27]:

$$\text{Removal MB (\%)} = \frac{C_0 - C_t}{C_0} \times 100 \quad \text{(Eq. 3)}$$

$$EEC = \left(\frac{UIt}{V}\right) \quad \text{(Eq. 4)}$$

where C_0 (MB concentration before EF process; mg L^{-1}), Ct (MB concentration after EF process; mg L^{-1}), U (applied voltage; V), I (electrical current; A), t (electrolysis time; h), and V (volume of sample;L).

2.4. Application of Response Surface Methodology

Response Surface Methodology (RSM) is a widely used mathematical and statistical approach employed to model, design, and evaluate the relationship between several independent variables and responses of the proposed model. The goal is to optimize the applied reaction in a short time and reduce the costs of the process. Unlike conventional methods for data analysis, RSM analyzes data using simple techniques based on the mathematical model. In the RSM, to optimize the studied variables, a polynomial function (often a quadratic polynomial model) can be used, as given in Equation 5 [27, 28]

$$Y = \beta_0 + \sum_{i=1}^{k} \beta_i X_i + \sum_{i=1}^{k} \beta_{ii} X_i^2 + \sum_{i=1}^{n-1} \sum_{j=i+1}^{k} \beta_{ij} X_i X_j \quad \text{(Eq. 5)}$$

where Y is the predicted response (MB removal %), k is the number of independent factors, β_0, β_i, β_{ii}, and β_{ij} are the constant, linear, quadratic, and interaction model coefficients, respectively, also, X_i, X_j, and ε are the independent factors and the error. Analysis of variance (ANOVA) with a 95% confidence interval was used to determine the significance of the parameters. In the current study, the RSM approach was used to investigate four variables' effects (initial MB concentration, H_2O_2 dosage, current density, and electrolysis time) and identify the optimal condition for MB removal using the EF process employing Design-Expert Software Version 11.0.4.0.

3. Result and discussion

3.1. Development of models and analysis of variance (ANOVA) using RSM

Table 1 describes the experimental condition of 30 runs designed by RSM and the obtained responses of the developed model in each run summarized. The mentioned removal efficiencies of MB are the averages of duplicate runs in each experimental condition.

Some valuable parameters, including lack of fit of the model, the significance of linear and interaction effects of operating variables, and coefficient of determination, were evaluated by analysis of variance (ANOVA). As seen in Table 2, the *p*-value less than 0.0001 corresponds to the significant coefficients.

As seen, the obtained results from ANOVA analysis confirmed that the developed quadratic regression model was satisfactorily fitted to the removal efficiency of the treatment process with the F-value of 858. Since the calculated *p*-value of the Lack of Fit was less than 0.05, it confirmed that the lack of fit was insignificant, corresponding to the pure error. The predicted and adjusted R^2 of 0.9915 and 0.9958 are in reasonable agreement. Furthermore, the fitted model's prediction ability over the experimental condition range is acceptable due to the obtained predicted R^2 of about 100%. The normality of the residuals was analyzed and demonstrated in Figure 1(a). As seen, all the demonstrated data are relatively near to a straight line with the R^2 of 0.9970. Moreover, the association between the obtained values of actual removal efficiencies and predicted removal efficiencies were revealed in Figure 1(b). As seen, since the residual results were distributed near the diagonal line, it can be concluded that the proposed treatment model successfully predicted the removal efficiencies.

Table 1. Experimental values for the removal efficiency of MB from the CCD.

Run order	Actual values				Coded values				Removal (%)
	A (mg L^{-1})	B (µL)	C (mA cm^{-2})	D (min)	X_1	X_2	X_3	X_4	
1	40	387	8.2	5.2	+1	+1	+1	-1	70.6
2	30	275	6.5	8.5	0	0	0	0	82.9
3	30	275	6.5	8.5	0	0	0	0	84.1
4	20	387	4.7	11.7	-1	+1	-1	+1	85.2
5	20	162	8.2	11.7	-1	-1	+1	+1	71.0
6	40	387	4.7	11.7	+1	+1	-1	+1	64.0
7	20	162	8.2	5.2	-1	-1	+1	-1	66.6
8	30	275	10.0	8.5	0	0	+2	0	67.2
9	20	387	4.7	5.2	-1	+1	-1	-1	82.3
10	10	275	6.5	8.5	-2	0	0	0	99.8
11	30	500	6.5	8.5	0	+2	0	0	77.1
12	30	50	6.5	8.5	0	-2	0	0	41.3
13	30	275	6.5	8.5	0	0	0	0	84.5
14	40	162	8.2	11.7	+1	-1	+1	+1	59.3
15	20	162	4.7	11.7	-1	-1	-1	+1	63.3
16	40	387	8.2	11.7	+1	+1	+1	+1	75.2
17	50	275	6.5	8.5	+2	0	0	0	69.8
18	30	275	3.0	8.5	0	0	-2	0	47.1
19	40	162	4.7	11.7	+1	-1	-1	+1	49.7
20	20	387	8.2	11.7	-1	+1	+1	+1	95.7
21	40	162	4.7	5.2	+1	-1	-1	-1	45.5
22	30	275	6.5	8.5	0	0	0	0	84.1
23	40	162	8.2	5.2	+1	-1	+1	-1	56.1
24	20	162	4.7	5.2	-1	-1	-1	-1	58.6
25	20	387	8.2	5.2	-1	+1	+1	-1	90.9
26	30	275	6.5	8.5	0	0	0	0	83.7
27	30	275	6.5	2.0	0	0	0	-2	67.5
28	30	275	6.5	15.0	0	0	0	+2	79.2
29	40	387	4.7	5.2	+1	+1	-1	-1	61.3
30	30	275	6.5	8.5	0	0	0	0	84.4

Table 2. ANOVA of the fitted polynomial model.

Source	Sum of Squares	Degree of freedom (df)	Mean square	F-value	p-value
Model	6580	8	822	858	< 0.0001
X_1	1535	1	1535	1602	< 0.0001
X_2	2142	1	2142	2237	< 0.0001
X_3	555	1	555	579	< 0.0001
X_4	125	1	125	130	< 0.0001
X_1X_2	72	1	72	76	< 0.0001
X_2^2	1087	1	1087	1135	< 0.0001
X_3^2	1276	1	1276	1332	< 0.0001
X_4^2	204	1	204	214	< 0.0001
Residual	20	21	0.96	-	-
Lack of Fit	18	16	1.15	3.54	0.0840
Pure Error	1.6	5	0.33	-	-
Core Total	6600	29	-	-	-
Mean: 71.65				R^2: 0.9970	
Coefficient of Variance: 1.37%				Adj.R^2: 0.9958	
Standard Deviation: 0.98				Pred. R^2: 0.9915	

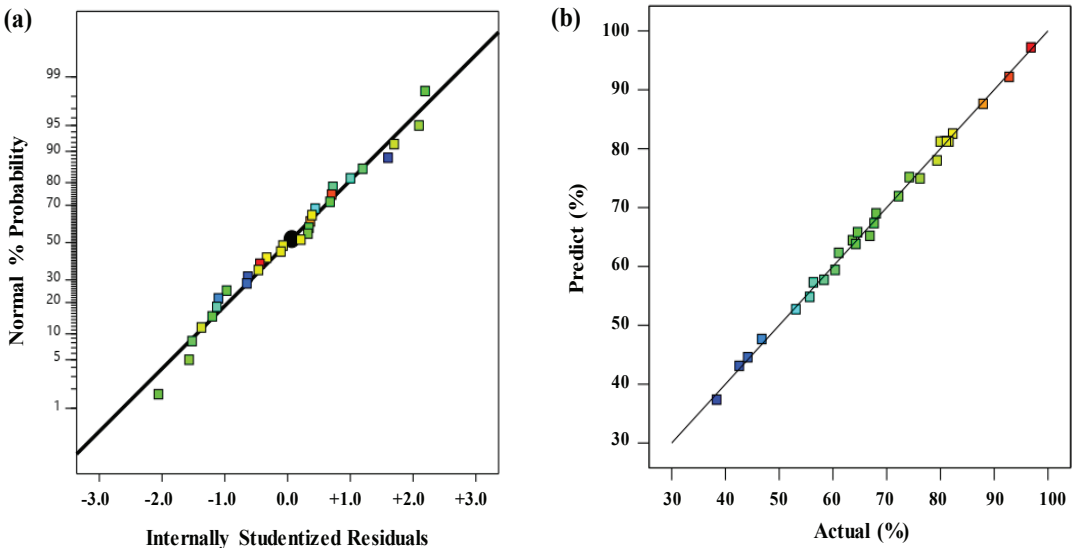

Fig. 1. **(a)** Normal probability plot of studentized residuals,
(b) Predicted removal efficiencies *vs.* experimental removal efficiencies.

The regression model developed for the removal efficiency of MB is represented in Equation 6. The proposed second-order model in the term of coded factors by eliminating the insignificant terms is expressed as follows (6):

$$MB\ removal\ (\%) = 84.2 - 8.9X_1 + 9.45X_2 + 4.81X_3 + 2.29X_4 - 2.13X_1X_2 - 6.23X_2^2 - 6.75X_3^2 - 2.71X_4^2 \quad \text{(Eq. 6)}$$

Here, X_1 represents initial MB concentration, X_2 is H_2O_2 dosage, X_3 is current density, and X_4 is electrolysis time. As seen, the intensity of each particular variable on the removal efficiency as the response of the proposed model is identified by the related magnitude of each variable's coefficient. Each coefficient's positive or negative value indicates the synergistic or antagonistic effect of the related variable on the response. As seen, the coefficients

of X_2 (H_2O_2 dosage), X_3 (current density), and X_4 (electrolysis time) are all positive. Moreover, it can be concluded that the variables of X_1 and X_2 with much larger coefficients play more significant roles in MB's removal efficiency as the model's response.

3.2. Effect of parameter on the MB removal efficiency

In the present study, the effect of initial MB dye concentration on removal efficiency using the EF process was investigated. As Figure 2 shows, the initial MB dye concentration is inversely related to the MB removal efficiency, when increasing the initial MB dye concentration from 10 mg L-1 to 500 mg L^{-1}, and removal efficiency decreases from 99.8% to 68.2%. This phenomenon can be due to the decrease in the ratio of oxidant agents to MB dye molecules. For example, if all the parameters studied in the EF process, are constant (at high MB dye concentrations), the number of dye molecules is greater than the oxidizing agents. Therefore, the number of oxidizing agents is insufficient to remove high concentrations of the dye molecule, and consequently, the removal efficiency decreases [29, 30].

Optimizing the amount of H_2O_2 in all treatment methods in which H_2O_2 plays a key role is very important because it affects the removal efficiency, the management of the treated effluent, and the cost. The effects of H_2O_2 dosage in the range of 50-500 µL on MB removal were investigated at the initial MB concentration of 30 mg L^{-1}, the current density of 6.5 mA cm^{-2}, and electrolysis time of 8.5 min, the result is shown in Figure 3 the obtained results show that the increase in degradation percentage from 40.7% to 78.1% whenever H_2O_2 increased from 50 to 500 µL, at the initial MB concentration of 30 mg L^{-1}, the current density of 6.5 mA cm^{-2}, and electrolysis time of 8.5 min.

Excess concentration of H_2O_2 causes the spontaneous auto composition of $H_2O_2$to H_2O and O_2 molecules through Equation(7), as well as the decomposition of $^{\bullet}OH$, produced during the EF reaction to radicals with lower oxidation strength ($HO_2^{\bullet}$ ions) according to Equation (8) and (9) which reduces the removal efficiency [31, 32].

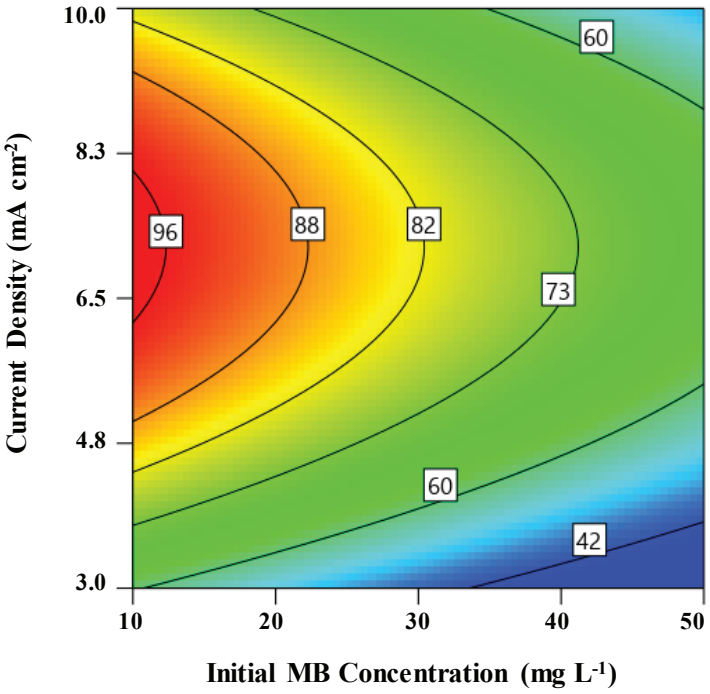

Fig. 2. Contour plots of the initial MB concentration and current density.

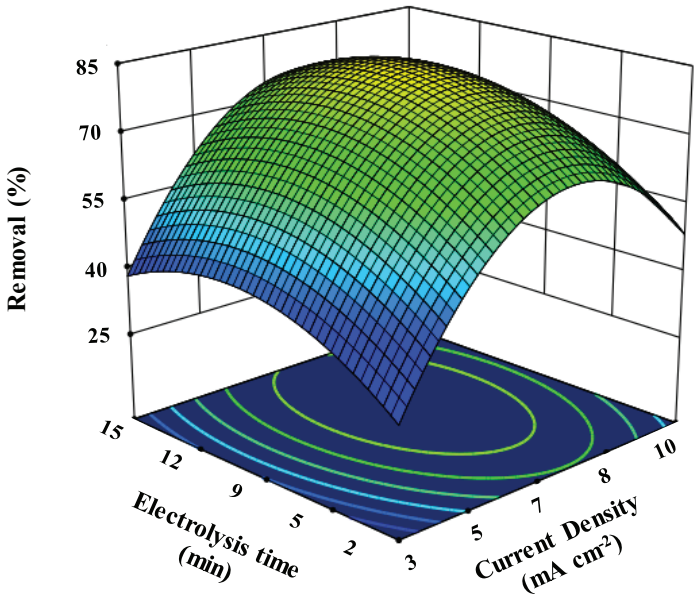

Fig. 3. 3Dplot of the initial MB concentration and H_2O_2 dosage.

$$2\,H_2O_2 \rightarrow 2H_2O + O_2 \quad \text{(Eq. 7)}$$

$$H_2O_2 + HO^{\bullet} \rightarrow HO_2^{\bullet} + H_2O \quad \text{(Eq. 8)}$$

$$HO_2^{\bullet} + HO^{\bullet} \rightarrow H_2O + O_2 \quad \text{(Eq. 9)}$$

Current density is one of the most effective parameters that affects the kinetic rate and removal efficiency. Increasing the current density more than the optimal value causes more electrical energy consumption and heat generation and consequently adverse effects on the removal process, so its value must be optimized. Due to the importance and influence of current density in the EF process, the effect of applied current density was studied in the range of 3-10 mA cm^{-2}. The removal of MB dye depended on the current density.

The increase in current density from 2 to 5.5 mA cm^{-2} offered faster MB dye degradation (MB removal efficiency of 47.5% to 66.9%). Increasing the dye removal efficiency with increasing current density can be attributed to the fact that increasing the current density increases the amount of iron generated by the anode electrode. The increase in removal and degradation rates from 3 mA cm^{-2} to the optimum value of 7.0 mA cm^{-2} can be related to the acceleration of Fenton's Reaction (Equation1). Therefore, increasing the concentration of Fe^{2+} produced could lead to an increase in $^{\bullet}OH$ generated through (Equation 1). These $^{\bullet}OH$ generated reacts immediately with the MB dye, increasing the MB removal efficiency.

However, more than the optimal value of current density leads to a decrease in the MB removal efficiency in the EF reactor. This negative effect is due to the role of Fe^{2+} as the scavenger of $^{\bullet}OH$ (Equation 10) [32, 33]. Hence, 7.0 mA cm^{-2} was selected as the optimal value of current density.

$$Fe^{2+} + HO^{\bullet} \rightarrow Fe^{3+} + OH^{-} \quad \text{(Eq. 10)}$$

The effect of electrolysis time in the range of 2-15 min on MB removal was studied (Fig. 4). According to the results; MB removal efficiency was directly related to electrolysis time, so with increasing electrolysis time, the removal efficiency increases. From the start EF process until 9 min after electrolysis time, due to in presence of sufficient H_2O_2 and Fe^{2+}, a large number of hydroxyl radicals ($^{\bullet}OH$) are generated according to the Fenton's reaction, which

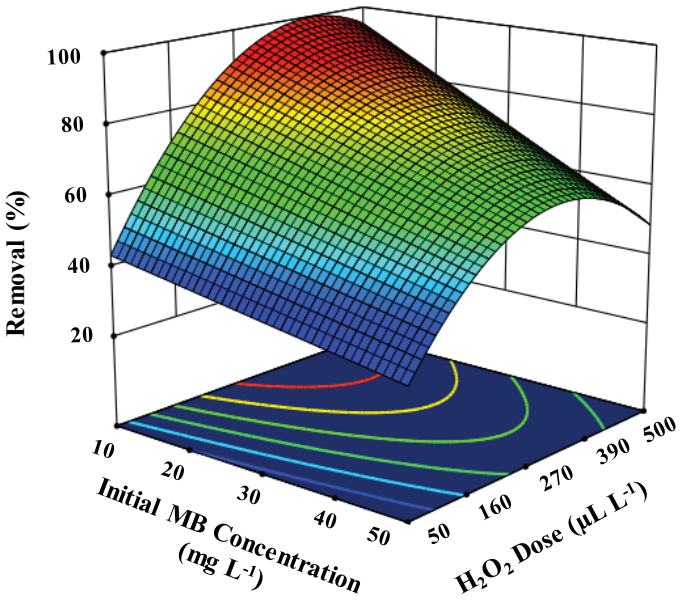

Fig. 4. The 3D plot of the current density and electrolysis time effects on the MB removal efficiency

subsequently leads to the MB dye degradation and increased removal efficiency. As the electrolysis time increases, the concentration of H_2O_2 in the electrochemical reactor decreases until the reactor is free of H_2O_2, consequently, the Fenton's reaction slows down and eventually stops [34].

3.3. Optimization process

The optimization process was carried out over the upper to lower limits of each operating parameter's value to determine the best treatment condition for maximum MB removal at a reasonable cost. The highest MB removal efficiency of 98.3% was predicted at the optimum condition of initial MB concentration of 20 mg L^{-1}, H_2O_2 dosage of 400 µL, the current density of 7.0 mA cm^{-2}, and electrolysis time of 10 min, which was in good accordance with the obtained experimental MB removal efficiency.

3.4. Kinetic model of hydroxide radical assisted EF process

The kinetic studies of the treatment process revealed that hydroxyl radical reaction with MB contaminant follows the pseudo-first-order reaction, which indicates that •OH directly attacked the contaminant molecules. The hydroxyl radicals are generated and consumed continuously at a similar rate to provide a steady-state concentration of active radicals throughout the treatment process. The apparent constant rate of K_{app} could be evaluated by the pseudo-first-order reaction equation and corresponds to the slope of demonstrated plot in Figure 5, with the value of 0.3753 min^{-1} [35]. Figure 5 revealed the variation of Ln (C_0/C_t) in the function of time during the 15 min treatment process with the initial concentration of MB 20 mg L^{-1}, the current density of 7.0 mA cm^{-2}, and H_2O_2 dosage of 400 µL L^{-1}.

4. Conclusion

Herein, to achieve an economical treatment process for the efficient removal of MB, the response surface methodology was employed. The analysis of variance (ANOVA) at the confidence level of 95% was carried out to evaluate the significance of the independent variables and their interactions. The obtained results revealed that the initial MB concentration and H_2O_2 dosage affected the removal efficiency significantly. The obtained experimental removal efficiency of 95.8% by the EF process was in satisfactory agreement with the predicted removal efficiency of 98.3% by the

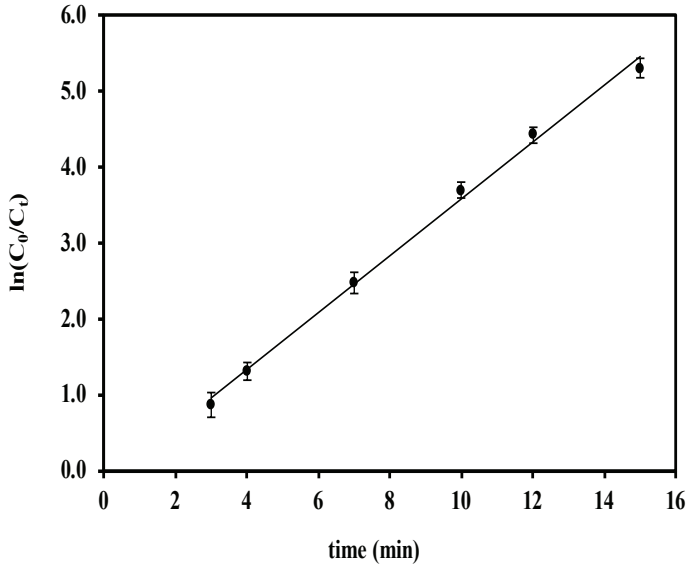

Fig. 5. Pseudo-first-order Kinetic model of MB degradation.

developed quadratic regression treatment model. The kinetic analysis showed that the applied treatment process followed a pseudo-first-order model.

5. Acknowledgements

The authors would like to express their appreciation to the student research committee of Kerman University of Medical Sciences [Grant number 400000747] for supporting the current work.

Funding: This work received a grant from the Kerman University of Medical Sciences [Grant number 400000747].

Conflict of interest: The authors declare that they have no conflict of interest regarding the publication of the current paper.

Ethical approval: The Ethics Committee of Kerman University of Medical Sciences approved the study (IR.KMU.REC.1400.510).

6. References

[1] S. Soni, P. Bajpai, J. Mittal, C. Arora, Utilisation of cobalt doped Iron-based MOF for enhanced removal and recovery of methylene blue dye from waste water, J. Mol. Liq., 314 (2020) 113642. https://doi.org/10.1016/j.molliq.2020.113642.

[2] H.N. Bhatti, Y. Safa, S.M. Yakout, O.H. Shair, M. Iqbal, A. Nazir, Efficient removal of dyes using carboxymethyl cellulose/alginate/polyvinyl alcohol/rice husk composite: adsorption/desorption, kinetics and recycling studies, Int. J. Biol. Macromol., 150 (2020) 861-870. https://doi.org/10.1016/j.ijbiomac.2020.02.093.

[3] J.-C. Lee, H.-J. Kim, H.-W. Kim, H. Lim, Iron-impregnated spent coffee ground biochar for enhanced degradation of methylene blue during cold plasma application, J. Ind. Eng. Chem., 98 (2021) 383-388. https://doi.org/10.1016/j.jiec.2021.03.026.

[4] I. Khan, K. Saeed, I. Zekker, B. Zhang, A.H. Hendi, A. Ahmad, S. Ahmad, N. Zada, H. Ahmad, L.A. Shah, Review on methylene blue: its properties, uses, toxicity and photodegradation, Water, 14 (2022) 242. https://doi.org/10.3390/w14020242.

[5] S.A. Almodaresi, M. Mohammadrezaei, M. Dolatabadi, M.R. Nateghi, Qualitative analysis of groundwater quality indicators based on Schuler and Wilcox diagrams: IDW and Kriging models, J. Environ. Health . Sustain. Dev., 4 (2019) 903 -912. https://doi.org/10.18502/jehsd.v4i4.2023

[6] M.B. Yeamin, M.M. Islam, A.-N. Chowdhury, M.R. Awual, Efficient encapsulation of toxic dyes from wastewater using several biodegradable natural polymers and their composites, J. Clean. Prod., 291 (2021) 125920. https://doi.org/10.1016/j.jclepro.2021.125920.

[7] M. Vakili, M. Rafatullah, B. Salamatinia, A.Z. Abdullah, M.H. Ibrahim, K.B. Tan, Z. Gholami, P. Amouzgar, Application of chitosan and its derivatives as adsorbents for dye removal from water and wastewater: A review, Carbohydrate polymers, 113 (2014) 115-130. https://doi.org/10.1016/j.carbpol.2014.07.007.

[8] A. Kirchon, P. Zhang, J. Li, E.A. Joseph, W. Chen, H.-C. Zhou, Effect of isomorphic metal substitution on the fenton and photo-fenton degradation of methylene blue using Fe-based metal–organic frameworks, ACS Appl. Mater. Interfaces, 12 (2020) 9292-9299. https://doi.org/10.1021/acsami.9b21408.

[9] A. Kausar, S.U. Rehman, F. Khalid, A. Bonilla-Petriciolet, D.I. Mendoza-Castillo, H.N. Bhatti, S.M. Ibrahim, M. Iqbal, Cellulose, clay and sodium alginate composites for the removal of methylene blue dye: Experimental and DFT studies, Int. J. Biol. Macromol., 209 (2022) 576-585. https://doi.org/10.1016/j.ijbiomac.2022.04.044.

[10] A. Bukhari, M. Atta, A. Nazir, M.R. Shahab, Q. Kanwal, M. Iqbal, H. Albalawi, N. Alwadai, Catalytic degradation of MO and MB dyes under solar and UV light irradiation using ZnO fabricated using Syzygium Cumini leaf extract, Zeitschrift für Physikalische Chem., 236 (2022) 659-671. https://doi.org/10.1515/zpch-2021-3096.

[11] A. Syafiuddin, M.A. Fulazzaky, Decolorization kinetics and mass transfer mechanisms of Remazol Brilliant Blue R dye mediated by different fungi, Biotechnol. Reports, 29 (2021) e00573. https://doi.org/10.1016/j.btre.2020.e00573.

[12] M. Ghazaghi, HZ. Mousavi, H. Shirkhanloo, A. Rashidi, Ultrasound assisted dispersive micro solid-phase extraction of four tyrosine kinase inhibitors from serum and cerebrospinal fluid by using magnetic nanoparticles coated with nickel-doped silica as an adsorbent, Microchim. Acta, 183 (2016) 2779-2789. https://doi.org/10.1007/s00604-016-1927-z

[13] H. shirkhanloo, M. Osanloo, Nobel method for toluene removal from air based on ionic liquid modified nano-graphen, Int. J. Occup. Hyg., 6 (2014) 1-5. https://ijoh.tums.ac.ir/index.php/ijoh/article/view/89

[14] M.B.H. Abadi, H. Shirkhanloo, J. Rakhtshah, Air pollution control: The evaluation of TerphApm@ MWCNTs as a novel heterogeneous sorbent for benzene removal from air by solid phase gas extraction, Arab. J. Chem., 13 (2020) 1741-1751. https://doi.org/10.1016/j.arabjc.2018.01.011

[15] A. Faghihi-Zarandi, H. Shirkhanloo, C. Jamshidzadeh, A new method for removal of hazardous toluene vapor from air based on ionic liquid-phase adsorbent, Int. J. Environ. Sci. Technol., 16 (2019) 2797-2808. https://doi.org/10.1007/s13762-018-1975-5

[16] C. Jamshidzadeh, H. Shirkhanloo, A new analytical method based on bismuth oxide-fullerene nanoparticles and photocatalytic oxidation technique for toluene removal from workplace air, Anal. Methods Environ. Chem. J., 2 (2019) 73-86. https://doi.org/10.24200/amecj.v2.i01.55

[17] R. Ashouri, H Shirkhanloo, AM Rashidi, SAH Mirzahosseini, N. Mansouri, Dynamic and static removal of benzene from air based on task-specific ionic liquid coated on MWCNTs by sorbent tube-headspace solid-phase extraction procedure, Int. J. Environ. Sci. Technol., 18 (2021) 2377-2390. https://doi.org/10.1007/s13762-020-02995-4

[18] F. Jamali-Behnam, A.A. Najafpoor, M. Davoudi, T. Rohani-Bastami, H. Alidadi, H. Esmaily, M. Dolatabadi, Adsorptive removal of arsenic from aqueous solutions using

magnetite nanoparticles and silica-coated magnetite nanoparticles, Environ. Prog. Sustain. Energy, 37 (2018) 951-960. https://doi.org/10.1002/ep.12751.

[19] A. Najafpoor, H. Alidadi, H. Esmaeili, T. Hadilou, M. Dolatabadi, A. Hosseinzadeh, M. Davoudi, Optimization of anionic dye adsorption onto Melia azedarach sawdust in aqueous solutions: effect of calcium cations, Asia-Pacific J. Chem. Eng., 11 (2016) 258-270. https://doi.org/10.1002/apj.1962.

[20] I. Sirés, E. Brillas, M.A. Oturan, M.A. Rodrigo, M. Panizza, Electrochemical advanced oxidation processes: today and tomorrow. A review, Environ. Sci. Pollut. Res., 21 (2014) 8336-8367. https://doi.org/10.1007/s11356-014-2783-1.

[21] M. Rezayi, L.Y. Heng, A. Kassim, S. Ahmadzadeh, Y. Abdollahi, H. Jahangirian, Immobilization of tris (2 pyridyl) methylamine in a PVC-Membrane Sensor and Characterization of the Membrane Properties, Chem. Cent. J., 6 (2012) 1-6. https://doi.org/10.1186/1752-153X-6-40.

[22] S. Ata, M. Feroz, I. Bibi, I.-u. Mohsin, N. Alwadai, M. Iqbal, Investigation of electrochemical reduction and monitoring of p-nitrophenol on imprinted polymer modified electrode, Synthetic Metals, 287 (2022) 117083. https://doi.org/10.1016/j.synthmet.2022.117083.

[23] Y. Zhu, R. Zhu, Y. Xi, J. Zhu, G. Zhu, H. He, Strategies for enhancing the heterogeneous Fenton catalytic reactivity: a review, Appl. Catal. B: Environ., 255 (2019) 117739. https://doi.org/10.1016/j.apcatb.2019.05.041.

[24] Y.S. Woo, M. Rafatullah, A.F.M. Al-Karkhi, T.T. Tow, Removal of Terasil Red R dye by using Fenton oxidation: a statistical analysis, Desalination Water Treat., 52 (2014) 4583-4591. https://doi.org/10.1080/19443994.2013.804454.

[25] M. Dolatabadi, M.T. Ghaneian, C. Wang, S. Ahmadzadeh, Electro-Fenton approach for highly efficient degradation of the herbicide 2, 4-dichlorophenoxyacetic acid from agricultural wastewater: Process optimization, kinetic and mechanism, J. Mol. Liq., 334 (2021) 116116. https://doi.org/10.1016/j.molliq.2021.116116.

[26] A. Talaiekhozani, M.R. Mosayebi, M.A. Fulazzaky, Z. Eskandari, R. Sanayee, Combination of TiO2 microreactor and electroflotation for organic pollutant removal from textile dyeing industry wastewater, Alexandria Eng. J., 59 (2020) 549-563. https://doi.org/10.1016/j.aej.2020.01.052.

[27] R.A. Khera, M. Iqbal, A. Ahmad, S.M. Hassan, A. Nazir, A. Kausar, H.S. Kusuma, J. Niasr, N. Masood, U. Younas, Kinetics and equilibrium studies of copper, zinc, and nickel ions adsorptive removal on to Archontophoenix alexandrae: conditions optimization by RSM, Desalination Water Treat., 201 (2020) 289-300. https://doi.org/10.5004/dwt.2020.25937.

[28] M. Dolatabadi, H. Naidu, S. Ahmadzadeh, A green approach to remove acetamiprid insecticide using pistachio shell-based modified activated carbon; economical groundwater treatment, J. Clean. Prod., 316 (2021) 128226. https://doi.org/10.1016/j.jclepro.2021.128226.

[29] M. López-Guzmán, M.A. Flores-Hidalgo, L. Reynoso-Cuevas, Electrocoagulation process: An approach to continuous processes, reactors design, pharmaceuticals removal, and hybrid systems—A Review, Processes, 9 (2021) 1831. https://doi.org/10.3390/pr9101831.

[30] P. Nidheesh, R. Gandhimathi, Trends in electro-Fenton process for water and wastewater treatment: an overview, Desalination, 299 (2012) 1-15. https://doi.org/10.1016/j.desal.2012.05.011.

[31] E. Brillas, S. Garcia-Segura, Benchmarking recent advances and innovative technology approaches of Fenton, photo-Fenton, electro-Fenton, and related processes: A review on the relevance of phenol as model molecule, Sep.

Purif. Technol., 237 (2020) 116337. https://doi.org/10.1016/j.seppur.2019.116337.

[32] J. Casado, Towards industrial implementation of Electro-Fenton and derived technologies for wastewater treatment: A review, J. Environ. Chem. Eng., 7 (2019) 102823. https://doi.org/10.1016/j.jece.2018.102823.

[33] H. Monteil, Y. Pechaud, N. Oturan, M.A. Oturan, A review on efficiency and cost effectiveness of electro-and bio-electro-Fenton processes: application to the treatment of pharmaceutical pollutants in water, Chem. Eng. J., 376 (2019) 119577. https://doi.org/10.1016/j.cej.2018.07.179.

[34] J.J. Rueda-Márquez, I. Levchuk, M. Manzano, M. Sillanpää, Toxicity reduction of industrial and municipal wastewater by advanced oxidation processes (Photo-Fenton, UVC/H2O2, Electro-Fenton and Galvanic Fenton): a review, Catalysts, 10 (2020) 612. https://doi.org/10.3390/catal10060612.

[35] A. Chmayssem, S. Taha, D. Hauchard, Scaled-up electrochemical reactor with a fixed bed three-dimensional cathode for electro-Fenton process: Application to the treatment of bisphenol A, Electrochim. Acta, 225 (2017) 435-442. https://doi.org/10.1016/j.electacta.2016.12.183.